

N 70 26098

NASA CR102615
T-70-00239

EQUIVALENT MECHANICAL MODEL OF PROPELLANT SLOSHING IN THE WORKSHOP CONFIGURATION OF THE SATURN S-IVB

by

Franklin T. Dodge
Luis R. Garza

FINAL REPORT

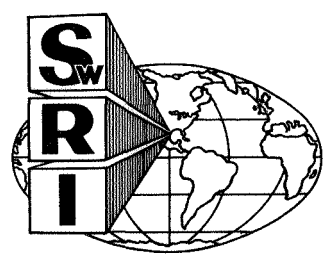
Contract NAS8-21478
Control No. DCN 1-8-75-00136(1F)
SwRI Project No. 02-2397

Prepared for

National Aeronautics and Space Administration
George C. Marshall Space Flight Center
Marshall Space Flight Center, Alabama 35812

June 1969

CASE FILE COPY



SOUTHWEST RESEARCH INSTITUTE
SAN ANTONIO HOUSTON

Handwritten signature

SOUTHWEST RESEARCH INSTITUTE
Post Office Drawer 28510, 8500 Culebra Road
San Antonio, Texas 78228

EQUIVALENT MECHANICAL MODEL OF PROPELLANT SLOSHING IN THE WORKSHOP CONFIGURATION OF THE SATURN S-IVB

by

Franklin T. Dodge
Luis R. Garza

FINAL REPORT

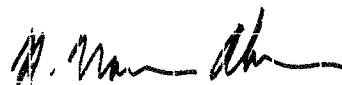
Contract NAS8-21478
Control No. DCN 1-8-75-00136(1F)
SwRI Project No. 02-2397

Prepared for

National Aeronautics and Space Administration
George C. Marshall Space Flight Center
Marshall Space Flight Center, Alabama 35812

June 1969

Approved:



H. Norman Abramson, Director
Department of Mechanical Sciences

ABSTRACT

An equivalent mechanical model was developed for propellant sloshing in the irregular compartmentation of the S-IVB workshop configuration during roll and lateral excitations. An experimental program employing scale-models yielded the data necessary to compute the mechanical model parameters for the eleven important slosh modes. The mechanical model was shown to give an excellent representation of the sloshing when the compartment doors are closed and a satisfactory representation when the doors are open. One important result is that nearly seven-tenths of the liquid participates in the rigid body motion of the tank during roll excitation.

ACKNOWLEDGMENT

The authors wish to thank the Technical Monitor, Mr. Harry J. Buchanan of the NASA-MSFC Aero-Astroynamics Laboratory, for several valuable discussions and liaison help with the prime contractor of the Workshop mission.

TABLE OF CONTENTS

Section	Title	Page
	LIST OF ILLUSTRATIONS	vi
	LIST OF PRINCIPAL SYMBOLS	vii
I	INTRODUCTION	1
II	MODELING CONSIDERATIONS	2
III	COMPARTMENT MECHANICAL MODELS FOR LATERAL EXCITATION	4
	Test Procedures and Data Reduction	5
	Mechanical Models	6
IV	MOMENT OF INERTIA FOR ROLL EXCITATION	18
	Test Procedures	18
	Equivalent Moment of Inertia	18
V	COMPARISON OF COMPLETE MECHANICAL MODEL WITH TESTS	20
	Lateral Excitation	20
	Roll Excitation	23
	Tests with the Liquid Level Above the Compartments	23
VI	CONCLUSIONS	26
VII	LIST OF REFERENCES	27

LIST OF ILLUSTRATIONS

Figure	Title	Page
1	Typical Mechanical Model for Cylindrical Tank	2
2	Main Scale-Model	4
3	Compartment Configuration in Main Scale-Model	4
4	Test Setup for Lateral Excitation Tests	5
5	Mechanical Model Parameters for Compartments 1 and 2	7
6	Mechanical Model Parameters for Compartment No. 3	9
7	Mechanical Model Parameters for Compartment No. 4	11
8	Mechanical Model Parameters for Compartment No. 5	13
9	Comparison of Mechanical Model to Tests for Compartment No. 5	15
10	Orientation of Mechanical Models for Complete Tank	17
11	Test Setup for Roll Excitation Tests	18
12	Polar Moment of Inertia with Doors Closed	19
13	Polar Moment of Inertia with Doors Open	19
14	Comparison of Mechanical Model for Complete Tank to Test Results—Lateral Excitation $x_o = 0.005$ in., Doors Closed	21
15	Comparison of Mechanical Model for Complete Tank to Test Results—Lateral Excitation $x_o = 0.005$ in., Doors Open	22
16	Comparison of Mechanical Model for Complete Tank to Test Results—Roll Excitation $\theta_o = 0.08^\circ$, Doors Closed	24
17	Comparison of Mechanical Model for Complete Tank to Test Results—Roll Excitation $\theta_o = 0.08^\circ$, Doors Open	24
18	Liquid Level Above Top of Compartments	24

LIST OF PRINCIPAL SYMBOLS

Symbol	Definition
F	lateral slosh force
f	excitation frequency
f_n	natural frequency of n^{th} mode
g	steady axial acceleration or gravity
h	liquid level above compartment bottom
h_n	height of slosh mass above compartment center-of-mass
$I_{\text{equivalent}}$	polar moment of inertia of liquid about tank axis
ℓ_n	perpendicular distance from the tank axis to the line of action of the n^{th} mode
M	slosh moment caused by lateral excitation
\mathcal{M}	total liquid mass in tank
m_n	slosh mass for n^{th} mode
m_o	rigidly attached mass in mechanical model for compartment
m_T	total liquid mass in compartment
R_o	radius of tank
T	slosh torque for roll excitation
t	time
x_o	amplitude of lateral excitation
γ_n	viscous damping coefficient for n^{th} mode
θ	direction of lateral excitation, see Figure 3
θ_n	direction of line-of-action of n^{th} mode
θ_o	amplitude of roll excitation
ν	kinematic viscosity of liquid
ρ	density of liquid
ω_n	equal to $2\pi f_n$

I. INTRODUCTION

The S-IVB stage of the SATURN V booster has proved to be a versatile research tool. For the projected AS-209 mission, the stage will be used as an orbiting workshop in which the liquid hydrogen tank is subdivided by reinforced fabric partitions into a series of irregular compartments. This compartmentation will substantially alter the sloshing characteristics of the propellant contained in the LH_2 tank during thrusting; further, the asymmetry of the tank makes the fluid susceptible to sloshing caused by roll excitation. Coupling of roll with sloshing for the S-IVB is a new problem and one that could seriously affect the vehicle's stability and control.

To investigate the propellant motions under such conditions, a comprehensive experimental program whose objective was to reduce the sloshing dynamics to an equivalent mechanical model of springs, masses, and dashpots has been conducted; because of the complexity and lack of axial symmetry of the compartmentation, a completely analytical program was ruled out. To achieve the objectives, experiments were designed to:

- (1) Determine the predominant slosh model for each of the tank compartments as a function of the orientation of lateral excitation;
- (2) Determine the slosh mass, slosh mass location, natural frequency, and damping of each important mode;
- (3) Determine the rotary inertia for roll excitation; and
- (4) Determine a mechanical model for sloshing excited by roll.

In particular, Items (3) and (4) were of interest because of a possible overloading of the control system caused by large sloshing torques about the roll axis.

Several previous experimental investigations of equivalent mechanical models for other boosters have been conducted. Sumner, Stofan, and Shamro [1]* determined, by tests with a scale-model, the mechanical analogy of sloshing in the CENTAUR liquid oxygen tank; later, Stofan [2] showed that this mechanical model agreed well with prototype tests. Sumner, Lacovic, and Stofan [3] formulated a mechanical model for liquid sloshing in the CENTAUR liquid hydrogen tank by experimental measurements, with particular emphasis on the effect of a large baffle designed to prevent venting of LH_2 . Eggleston [4] determined the parameters of an equivalent mechanical model for the ATLAS fuel tank when the liquid level was near the shear membrane, a point at which the model derived analytically failed to give a valid representation. Other experimental programs are reviewed [5] and [6]. All of these studies, however, pertain to tanks that were substantially axisymmetric (hence, the pitch and yaw axes were indistinguishable, and the sloshing was not a function of the orientation of the lateral motion of the tank) and, further, the tanks were not susceptible to roll excitation. Because of these differences, the program described herein utilized experimental data to a much greater extent in deducing not only the model parameters but also the form of the model than was necessary in the programs mentioned above.

*Numbers in brackets refer to the List of References, Section VII.

II. MODELING CONSIDERATIONS

The experimental program was based upon the assumption that the sloshing forces and torques can be duplicated by an equivalent mechanical model. The validity of this assumption, as well as its limitation to linear systems, is shown in Ref. 6; this point will not be further elaborated upon here.

However, the use of small models to derive prototype data when certain of the governing dimensionless parameters are "out-of-scale" between model and prototype requires some discussion. It has been shown (see [7], for example) that tests using small models will exactly represent the sloshing in large prototypes whenever all the following dimensionless ratios for the model and the prototype are equal:

- (1) ℓ/R_o (*geometric similarity*) where ℓ is any linear dimension and R_o is some characteristic dimension, say, the radius of the tank.
- (2) $f^2 R_o/g$ (*kinematic or Froude number similarity*) where f is a characteristic frequency and g is a linear acceleration, say, thrust or gravity. (If no meaningful frequency can be defined, then f should be replaced by $1/\tau$ where τ is a significant or characteristic time.)
- (3) $R_o^2 f/\nu$ (*dynamic or Reynolds number similarity*) where ν is the kinematic viscosity of the liquid.
- (4) X_o/R_o (*excitation similarity*) where X_o either is the amplitude of a lateral excitation, x_o , or else is $\ell\theta_o$ where θ_o is the amplitude of a rotational excitation.

If these relations are equal for model and prototype, then the slosh forces and moments scale directly as the Euler number. That is, the dimensionless ratios $F/\rho X_o f^2 R_o^3$ and $M/\rho X_o f^2 R_o^4$ for model and prototype are equal for the same dimensionless frequency, $f^2 R_o/g$. The chief restrictions on this kind of modeling are: surface tension forces must be negligible (that is, the liquid must not be in a low-gravity environment) and the tank must be essentially rigid.

The primary *disadvantage* of modeling the slosh forces and moments themselves as outlined above lies in the requirement of Reynolds number similarity; it is generally difficult to make the Reynolds number of the scale-model and the prototype equal. Since the peak forces and moments at resonances are a strong function of the damping (that is, of the Reynolds number), some way of accounting for differences in the Reynolds number must be determined as part of the tests. It is here that the primary *advantage* of experimentally determining the parameters of an equivalent mechanical model becomes evident. The force and moment response of the scale-model tests can be used to determine mechanical model parameters which, when suitably nondimensionalized, are valid for both model and prototype, regardless of the exact value of the Reynolds number in either the model or the prototype, so long as the damping is not too large in either.

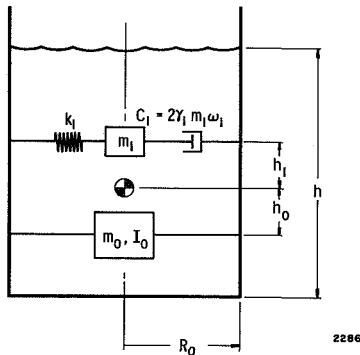


Figure 1. Typical Mechanical Model for Cylindrical Tank

A typical equivalent mechanical model for sloshing in the fundamental mode in a cylindrical tank is shown in Figure 1. For a lateral excitation of, say, $x_o e^{2\pi i f t}$ ($i = \sqrt{-1}$), the force exerted on the tank walls by either the sloshing or the equivalent system of masses, springs, and dashpots is

$$F = - (2\pi f)^2 x_o \left\{ m_o + m_1 \frac{\left(\frac{f}{f_1} \right)^2}{1 - \left(\frac{f}{f_1} \right)^2 + 2i\gamma_1 \left(\frac{f}{f_1} \right)} \right\} e^{2\pi i f t} \quad (1)$$

Consequently, a set of data of F versus f obtained experimentally with the scale-model allows f_1 , m_1 (and $k_1 = 4\pi^2 f^2 m_1$), γ_1 , and

m_o ($m_o = m_T - m_1$, where m_T is the total liquid mass) to be determined. Likewise, a moment-response curve allows h_1 to be determined. If a pitching excitation is used, then the equivalent moment of inertia of the liquid can also be determined. Further, these parameters are independent of the exact form of the time dependency of the excitation (random, sinusoidal, etc.); thus, the simplest kind of excitation, usually sinusoidal, may be used in the scale-model studies.

Once these results are obtained, it is easy to show by comparison to existing theories or by similitude analysis that the equivalent mechanical model parameters for scale-model and prototype are equal in the following dimensionless form:

- Slosh masses, m_n/m_T
- Rigidly attached masses, m_o/m_T
- Location of slosh masses, h_n/h
- Location of rigidly attached mass, h_o/h
- Slosh natural frequencies, $f_n^2 R_o/g$
- Damping parameters, $\gamma_n/\nu^{0.5} R_o^{-0.75} g^{-0.25}$

The only requirement between scale-model and prototype is geometric similarity, that is, equality of h/R_o . However, the particular form of nondimensionalizing the damping coefficients implies that there are no baffles or other significant flow obstructions protruding from the walls of the tank; if there are, then a “drag” form of nondimensionalizing should be used [8].

It can thus be seen that equivalent mechanical models, besides being very convenient in accounting for the influence of sloshing on a vehicle’s stability and control, allow scale-model data to be used more readily for prototype purposes.

III. COMPARTMENT MECHANICAL MODELS FOR LATERAL EXCITATION

A simple harmonic lateral excitation was used in the first series of tests, which were designed to provide the information required in formulating an equivalent mechanical model for each compartment. For this purpose, a completely compartmented scale-model tank (shown in Figure 2) and larger scale-models of the two rectangular and two wedge-shaped compartments in the S-IVB were built; the larger models resulted in larger and, therefore, more easily measured slosh forces and torques for these smaller compartments.

The dimensions of the main model shown in Figure 2 (scale factor = 1/14.8 of full size) are given in Figure 3. Compartments 1 and 2 are for waste and food storage, Compartments 3 and 4 are the crew

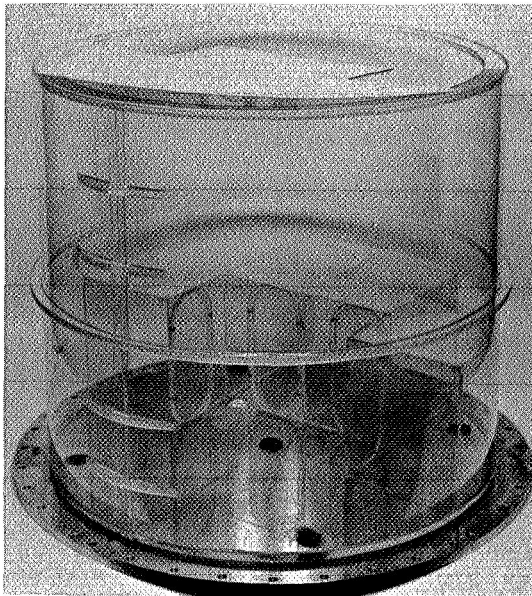


Figure 2. Main Scale-Model

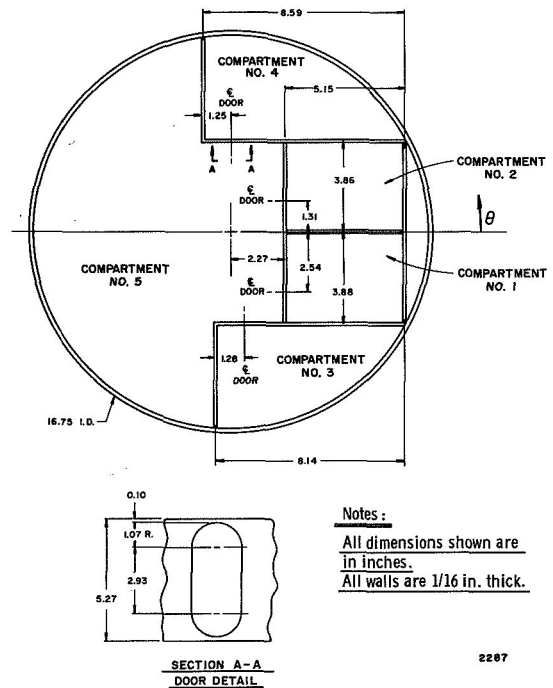


Figure 3. Compartment Configuration in Main Scale-Model

quarters, and Compartment 5 is the experimental laboratory. The proportion of the total liquid in the tank contained in each compartment for a given liquid level is:

- Compartment 1 or 2 = 9.03%
- Compartment 3 = 12.15%
- Compartment 4 = 13.22%
- Compartment 5 = 54.00%

The remaining 2.57% is contained in the cylindrical segment adjacent to Compartments 1 and 2; the sloshing in this compartment is negligible.

During thrusting, the "ceiling" of the workshop is the "floor" of the tank. (The thrusting configuration is the one for which a mechanical model is desired.) Since the ceiling is reinforced fabric containing a large number of small drain holes, the tank floor during thrust appears rigid for the sloshing motions; thus, the scale-model has a rigid aluminum base. Likewise, the "floor" of the workshop, which is an open gridwork of small girders except for reinforced fabric in Compartments 1 and 2, is the "ceiling" of the tank during flight, and, thus, the scale-model has no roof except over Compartments 1 and 2. The partitions in the S-IVB are reinforced fabric, but, for sloshing, they are sufficiently rigid that it is valid to use rigid plastic walls in the model.

The doorways shown in the model (there were no doorways in the larger models of Compartments 1, 2, 3, and 4) could be left either open or closed by tightly fitting doors. In flight, it is expected that the fabric doors will remain open to insure proper draining. Nevertheless, during the tests used to derive mechanical models, *the doors were closed* in order to isolate each compartment. As will be seen, the results still compare fairly well with tests in which the doors are open.

Test Procedures and Data Reduction

In any single model test, only one compartment contained liquid, the main model being used for Compartment 5 and the larger individual models for Compartments 1 or 2, 3, and 4. For each compartment, three levels of liquid (water) were examined— $1/4$, $1/2$, and $3/4$ of the total compartment height. For each liquid level, at least two different excitation amplitudes were used so that possible nonlinearities in the liquid's response might be evaluated. Figure 4 shows a typical experimental setup. The dynamometer-excitation system for measuring the slosh forces, moments, and excitation frequency and displacement is the same as that described in [9]; similar test procedures and data reductions were also used. Briefly, the excitation system consists of a massive shake table driven by a slider-crank mechanism through a variable-speed electric motor. The motor turns the driver crank, which is the large eccentric cam that can be seen in the lower left-hand corner of Figure 4.

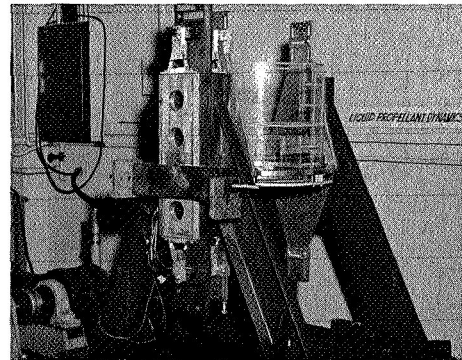


Figure 4. Test Setup for Lateral Excitation Tests

By altering the eccentricity of the cam-connecting rod arrangement, the amplitude of motion of the shake table (the slider in the slider-crank mechanism) can be varied. The frequency of the motion of the shake table is varied by changing the motor speed. The dynamometer is a system of tension-compression links (the wedge-shaped arms at the top and bottom of the aluminum bar in Figure 4) to which strain gages have been bonded. Depending on the electrical connection of the strain gages, the dynamometer senses either the lateral force or the pitching moment, or both, as in the tests described here. The strain gage signals are amplified, filtered, and then recorded on a strip chart. This system yields high quality, accurate, reproducible data.

The directions of excitation giving the largest sloshing motions for each compartment were determined by a brief series of tests in which the direction of the lateral excitation was varied by rotating the compartment and its aluminum base in the dynamometer-excitation apparatus, and in which the excitation frequency was varied over a wide range. Then, detailed data were obtained for those directions giving the largest sloshing motions as well as for one other direction, to be used later for comparison.

The force and moment data were plotted graphically with excitation frequency as the independent variable. A smooth curve drawn through the data points was used to compute the apparent damping by a half-bandwidth technique. (The various slosh modes in any one compartment were sufficiently well separated in frequency that coupling between the modes did not influence the results.) The damping parameter obtained from either the force or the moment response curve was usually the same; in the few

cases that more than a 10% discrepancy existed, the force response data were assumed to be the more accurate. Knowing the damping coefficient, γ_n , and the natural frequency, f_n (which, since the damping is small, is the frequency at which the maximum response occurs), the slosh mass, m_n , was obtained by matching the predicted peak force amplitude from Equation (1) to the measured peak. Other procedures to calculate m_n might have been used, but this one has the virtue of simplicity.

Knowing γ_n , f_n , and m_n , the location of the slosh mass, h_n above the center-of-mass was computed from the moment equation for the model:

$$M = -(2\pi f)^2 x_o m_n h \left\{ \frac{\frac{g}{(2\pi f)^2 h} + \left(\frac{h_n}{h}\right) \left(\frac{f}{f_n}\right)^2}{1 - \left(\frac{f}{f_n}\right)^2 + 2i\gamma_n \left(\frac{f}{f_n}\right)} \right\} e^{2\pi i f t} \quad (2)$$

by matching the predicted peak moment and the measured peak.

Upon comparing the results obtained at different excitation amplitudes, little or no nonlinearity (that is, dependence upon x_o) was found for either f_n or m_n ; however, h_n and γ_n did vary somewhat with x_o , and, thus, only the data for the smallest value of x_o were used in deriving the mechanical model parameters. This minimum value of 0.005 in. for x_o was about the smallest one that gave reducible data.

Mechanical Models

The mechanical model parameters obtained as outlined above for each compartment are shown in Figures 5 through 8. In every case, the mechanical model for a compartment is one or more spring-mass-dashpot oscillators and one rigidly attached mass.

Since an analytical model exists for rectangular tanks [6], the parameters for Compartments 1 and 2 may be compared to known results, as shown in Figure 5. (The small differences in the size of Compartments 1 and 2 are neglected here.) There are only trivial discrepancies between theory and experiment for the natural frequency and the slosh mass. A maximum discrepancy of about 25% in h_n exists for small liquid levels, which is undoubtedly due to the nonlinearities mentioned earlier*; fortunately, the difference between the moments is not of this magnitude since the moment is not directly proportional to h_n , as can be seen from Equation (2). The overall rather close correlation between the test results and the known theory demonstrates that the experimental methods used were sound.

In the figures, the tank radius, R_o , is the significant length used for nondimensionalizing both the natural frequency, which is presented in terms of the circular frequency, ω_n , to be consistent with the bulk of the existing literature, and the damping coefficient for all the compartments. Further, the slosh mass is presented both as a fraction of the liquid mass m_T contained within the compartment in question and as a fraction of the liquid in the complete tank, $\pi\rho R_o^2 h$, for the same liquid level. This should facilitate use of the curves in practice.

The slosh mass and frequency curves for the fundamental mode in a compartment were drawn through the data points in such a way that whenever possible the natural frequency approached zero and the slosh mass ratio with respect to m_T approached one as the liquid level approached zero. The reasoning behind this is that these two observations are true for every model, known to the authors, that has been derived analytically.

Comparisons of the predictions of the mechanical model for Compartment 5, as an example, and the test data are shown in Figure 9. Figure 9a illustrates the case of an excitation oriented in the direction $\theta = 90^\circ$ (see Figure 3 for the definition of θ). The mode excited here, which is called the first mode in Figure 8,

*Negative values of h_n mean that the slosh mass is located below the compartment center-of-mass.

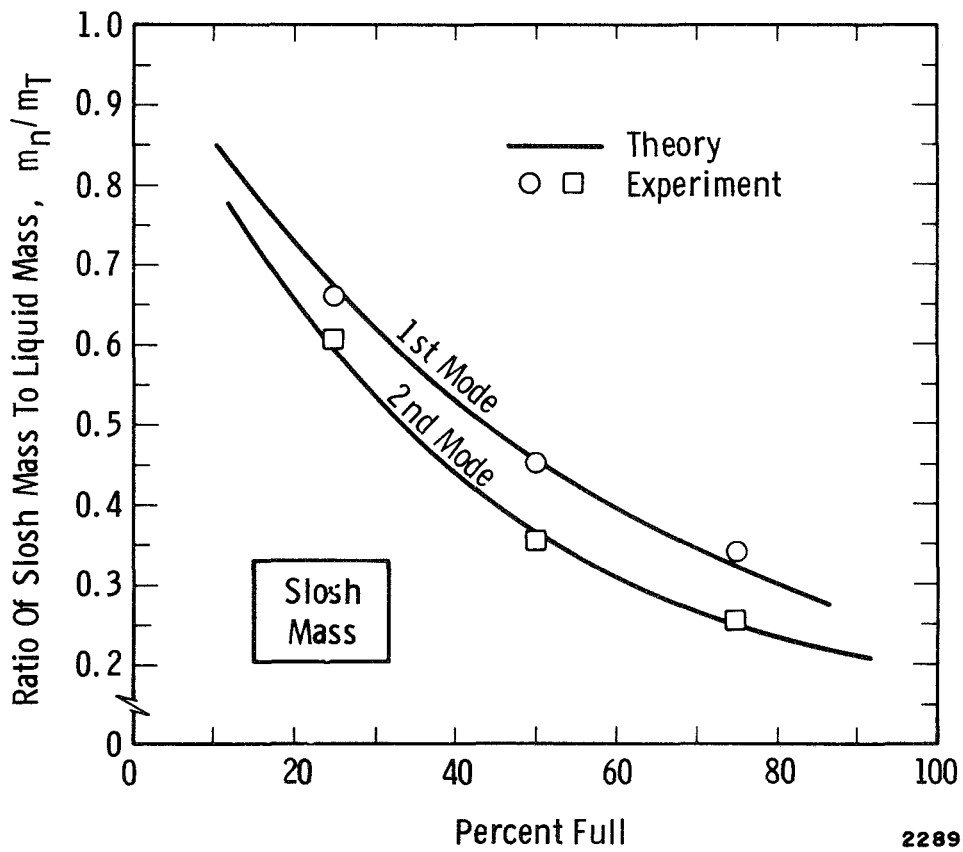
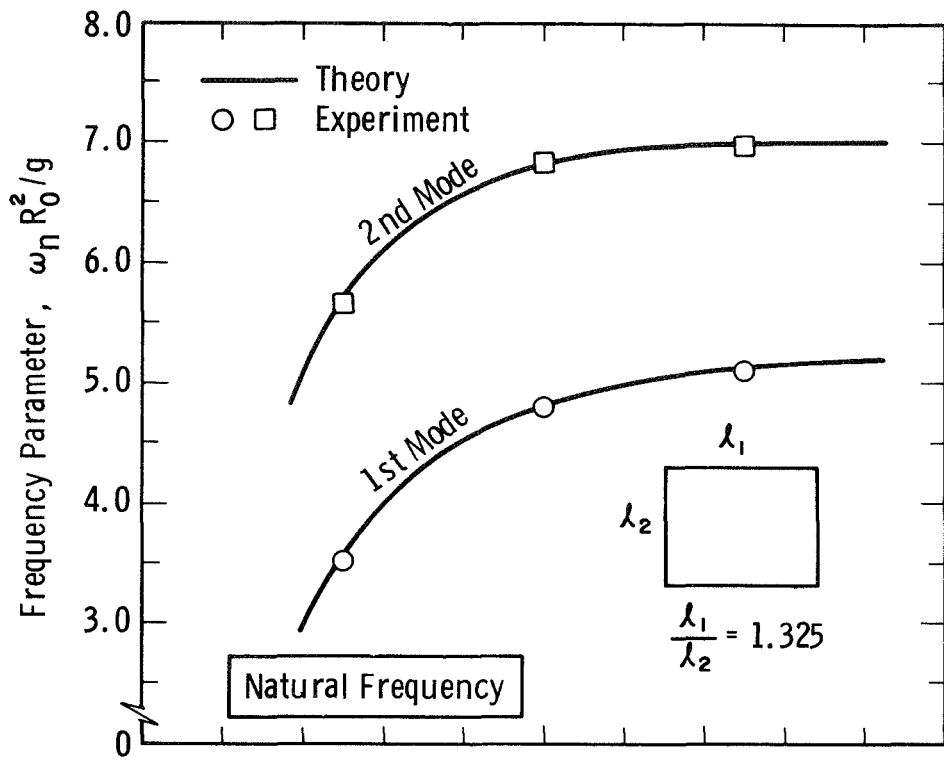


Figure 5. Mechanical Model Parameters for Compartments 1 and 2 (Cont'd)

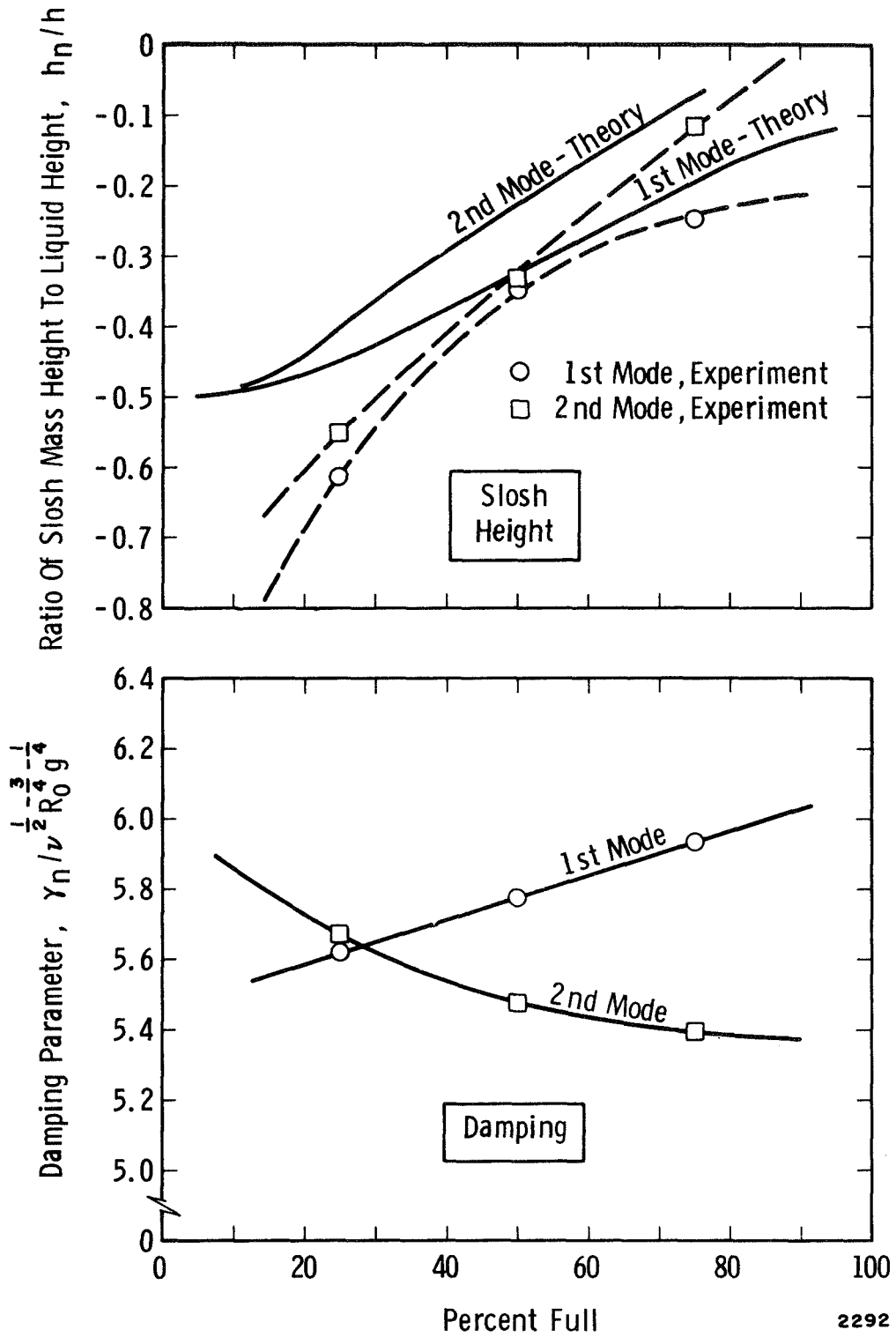


Figure 5. Mechanical Model Parameters for Compartments 1 and 2 (Concl'd)

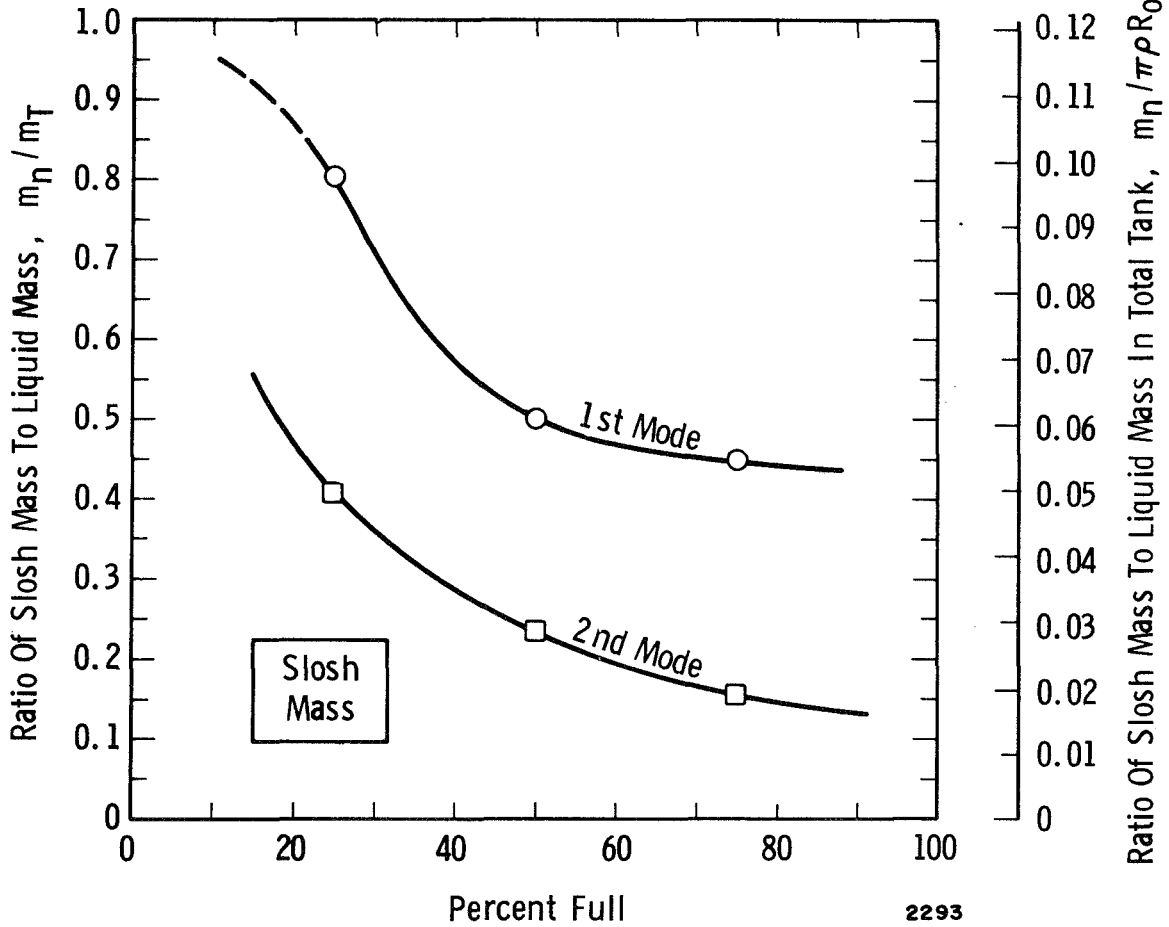
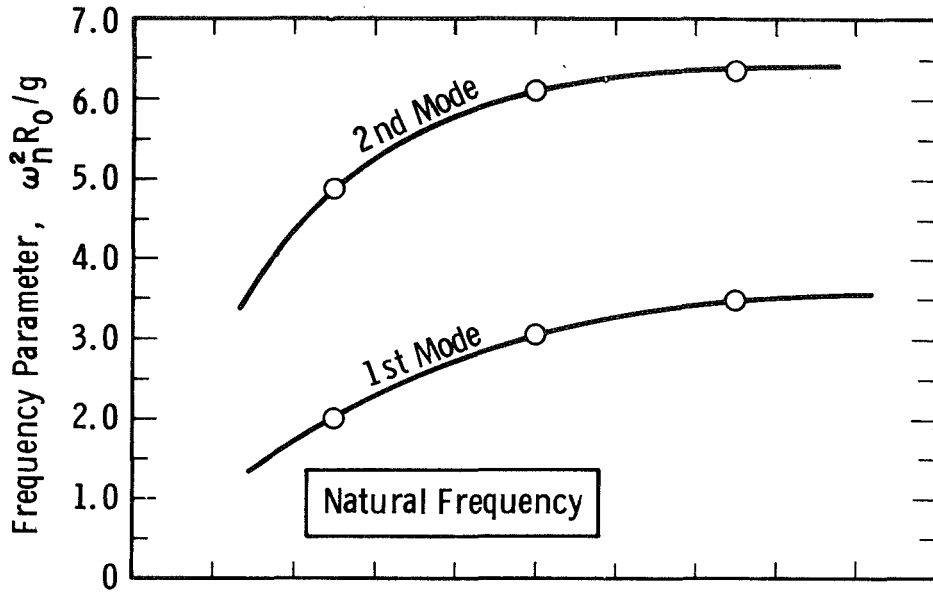


Figure 6. Mechanical Model Parameters for Compartment No. 3 (Cont'd)

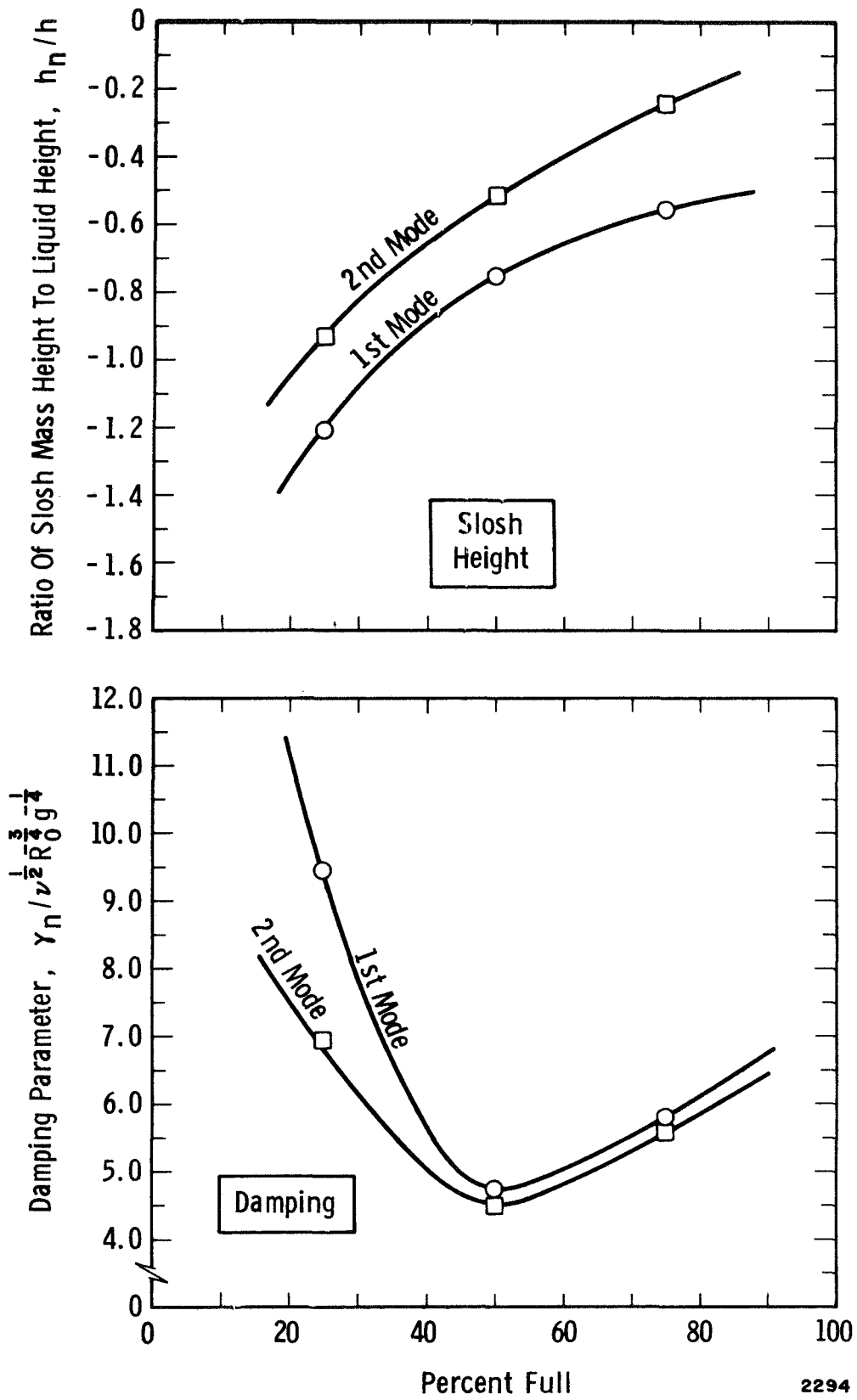
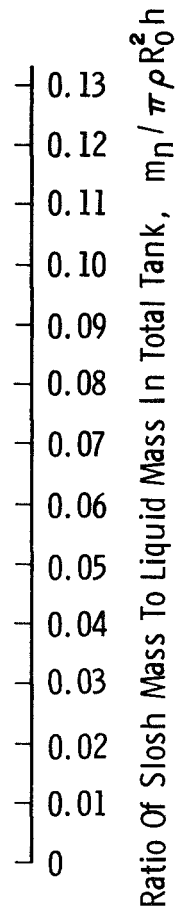
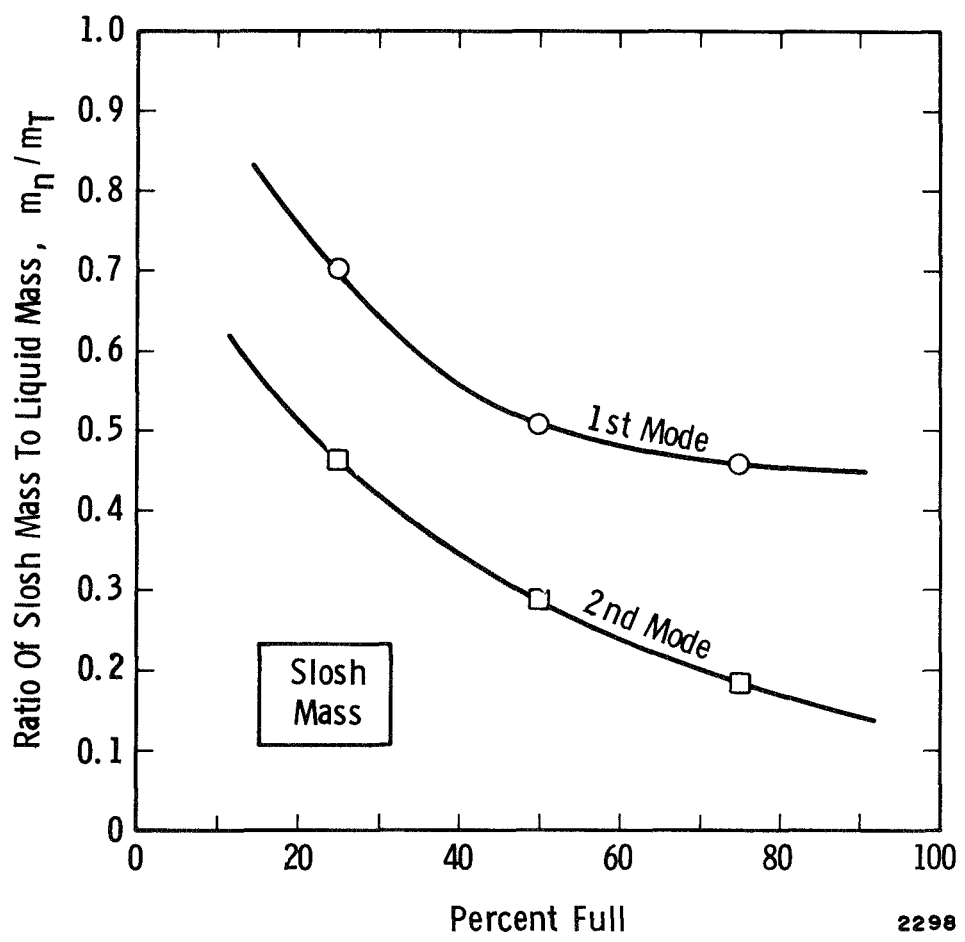
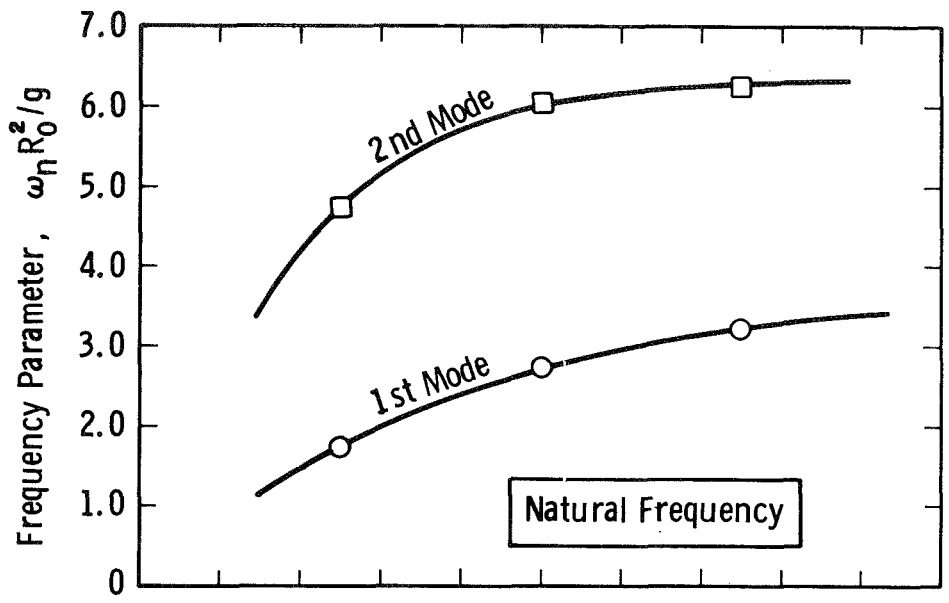


Figure 6. Mechanical Model Parameters for Compartment No. 3 (Concl'd)



2298

Figure 7. Mechanical Model Parameters for Compartment No. 4 (Cont'd)

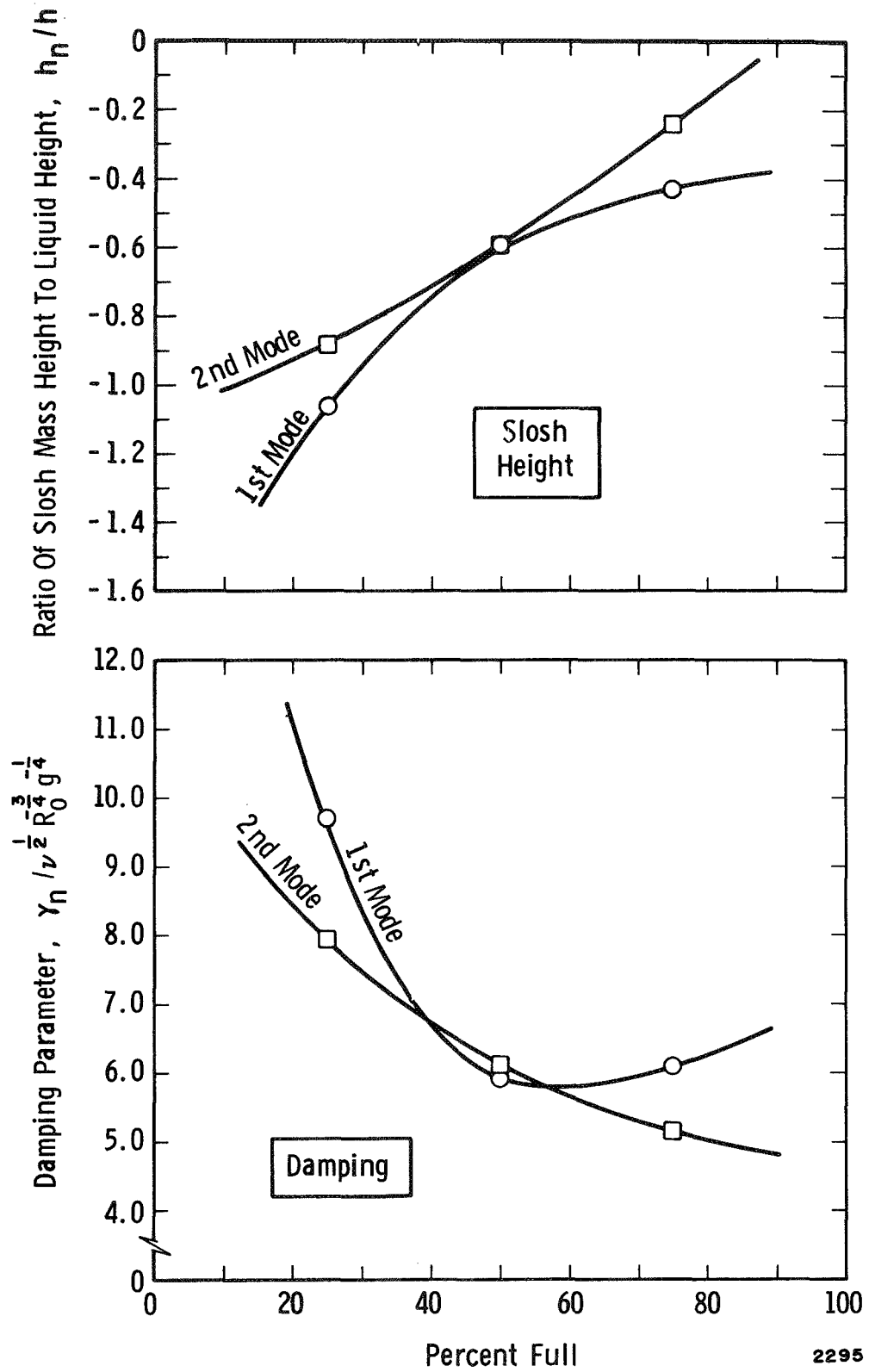


Figure 7. Mechanical Model Parameters for Compartment No. 4 (Concl'd)

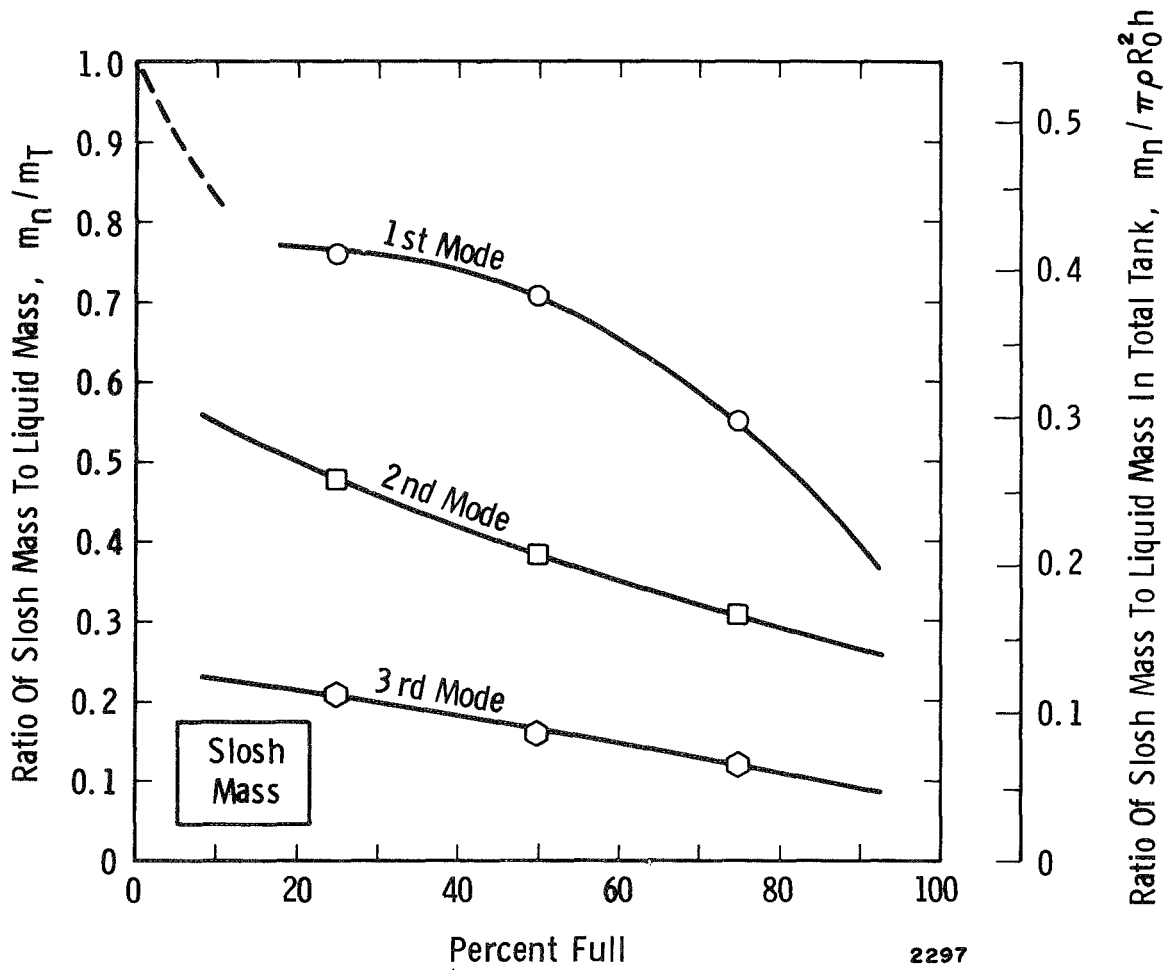
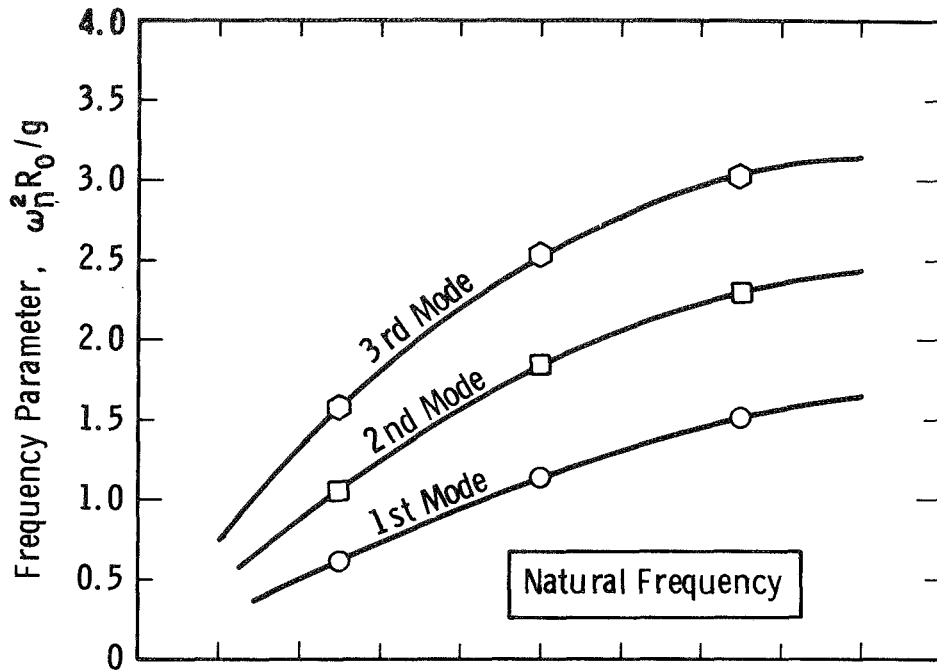


Figure 8. Mechanical Model Parameters for Compartment No. 5 (Cont'd)

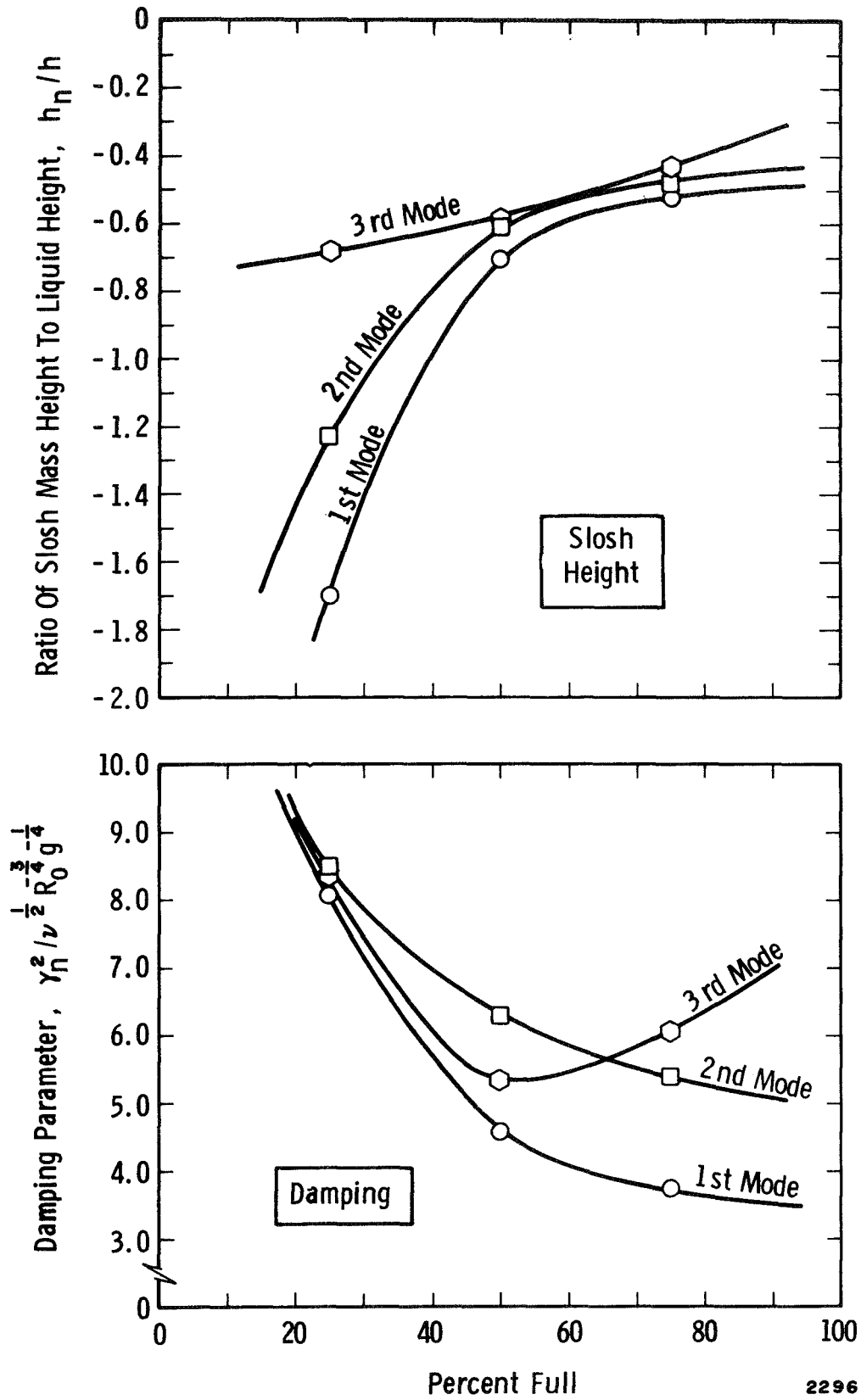
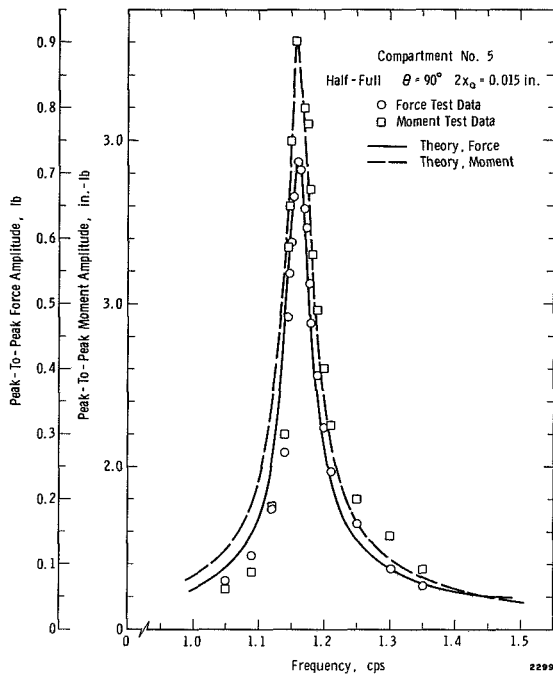
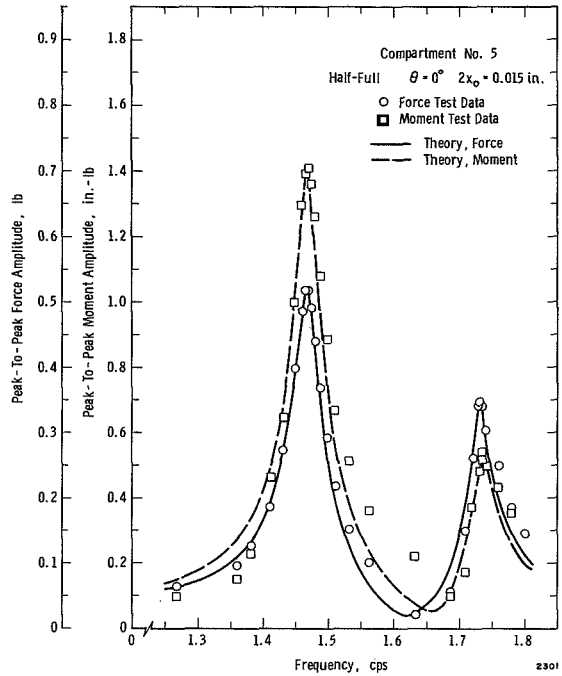


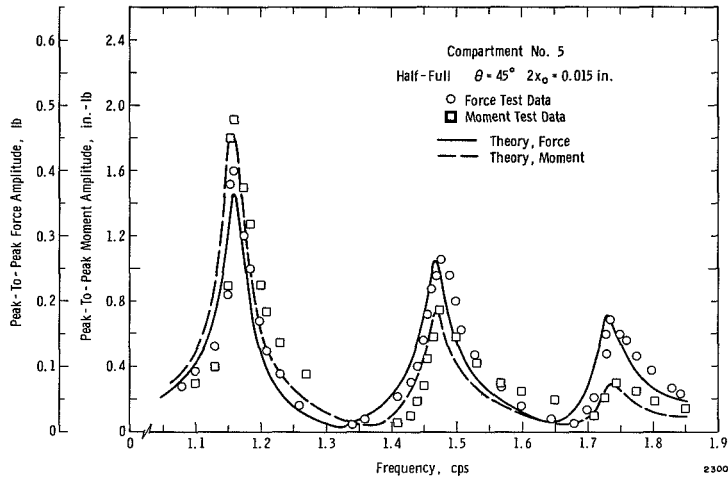
Figure 8. Mechanical Model Parameters for Compartment No. 5 (Concl'd)



a. Direction of Excitation = 90°



b. Direction of Excitation = 0°



c. Direction of Excitation = 45°

Figure 9. Comparison of Mechanical Model to Tests for Compartment No. 5

is very similar to the fundamental mode in a complete cylindrical tank. The direction $\theta = 90^\circ$ is the direction which excites this mode most strongly, and, furthermore, no other significant modes are excited. The comparison of the force and moment is very close, as indeed it should be since the mechanical model parameters for this mode were derived from data for $\theta = 90^\circ$ although for a smaller excitation amplitude. Corresponding comparisons for the modes produced when the excitation is along $\theta = 0^\circ$ are shown in Figure 9b. Two modes, called the second and third modes in Figure 8, predominated for $\theta = 0^\circ$, neither of which were produced when the excitation was along $\theta = 90^\circ$ nor was the predominant mode for $\theta = 90^\circ$ produced when $\theta = 0^\circ$. The comparison of theory and test is also close here since, once again, these model parameters were derived from data for $\theta = 0^\circ$. An independent verification is shown in Figure 9c, which

illustrates the case when the excitation is along $\theta = 45^\circ$, a direction that excites all three modes. Nevertheless, the comparison is still very close.

The arrangement of the spring-mass-dashpot oscillators for all the important modes in the complete tank is shown in Figure 10. The cross-hatched circles represent the slosh masses, although, in the undisturbed position, all the masses in any compartment lie directly over the center-of-mass (symbolized by \bullet); they are shown displaced in this sketch merely for clarity.

Compartments 4 and 5 are unique in the sense that there is not a direction of excitation that excites only one of the two principal modes; that is, the included angle between the two spring-dashpots is not 90° . This fact caused no particular problems in the tests since the natural frequencies of the two modes (see Figures 6 and 7) are widely separated.

There is only one rigidly attached mass, m_o , for each compartment. Since $m_o = m_T - \sum m_n$, m_o may be negative for some compartments, but this is not a real drawback. Only the part of the lateral excitation parallel to the line of action of the spring dashpot causes oscillations; the part perpendicular to it causes rigid body motions of the slosh masses, and, thus, the total mass acting as a rigid body is always positive. For example, suppose that the slosh force for Compartment 5 is desired, for an excitation of $x_o e^{2\pi ift}$ oriented at θ degrees to the zero-degree axis. Then, the force resolved in the direction of the excitation is

$$F = -(2\pi f)^2 x_o e^{2\pi ift} \left[m_o + m_1 \sin^2(\theta - 90^\circ) \right] + (4\pi f_1 m_1 \gamma_1 \dot{x}_1 + k_1 x_1) \cos(\theta - 90^\circ) \\ - (2\pi f)^2 x_o e^{2\pi ift} \left[(m_2 + m_3) \sin^2 \theta \right] + \sum_{n=2}^3 (4\pi f_n m_n \gamma_n \dot{x}_n + k_n x_n) \cos \theta \quad (3)$$

where x_n is the displacement of the mass m_n with respect to the tank. The equation of motion for the slosh masses is

$$m_n \ddot{x}_n + 4\pi f_n m_n \gamma_n \dot{x}_n + k_n x_n = (2\pi f)^2 x_o m_n \cos(\theta - \theta_n) e^{2\pi ift} \quad (4)$$

where θ_n is the direction of the line of action of the n^{th} spring dashpot. Solving Equation (4) for the steady-state x_n and then substituting it into Equation (3) shows that the slosh force in the θ direction is

$$F = -(2\pi f)^2 x_o e^{2\pi ift} \left\{ m_o + \sum_{n=1}^3 m_n + \sum_{n=1}^3 m_n \cos^2(\theta - \theta_n) \left[\frac{\left(\frac{f}{f_n}\right)^2}{1 - \left(\frac{f}{f_n}\right)^2 + 2i\gamma_n \left(\frac{f}{f_n}\right)} \right] \right\} \quad (5)$$

which, since $m_o + \sum_{n=1}^3 m_n = m_T$, is the correct equation. There is also a slosh force in the direction $\theta + 90^\circ$,

which can be obtained from Equation (5) by dropping the $m_o + \sum_{n=1}^3 m_n$ term and by replacing $\cos^2(\theta - \theta_n)$ in the last term with $\sin(\theta - \theta_n) \cos(\theta - \theta_n)$.

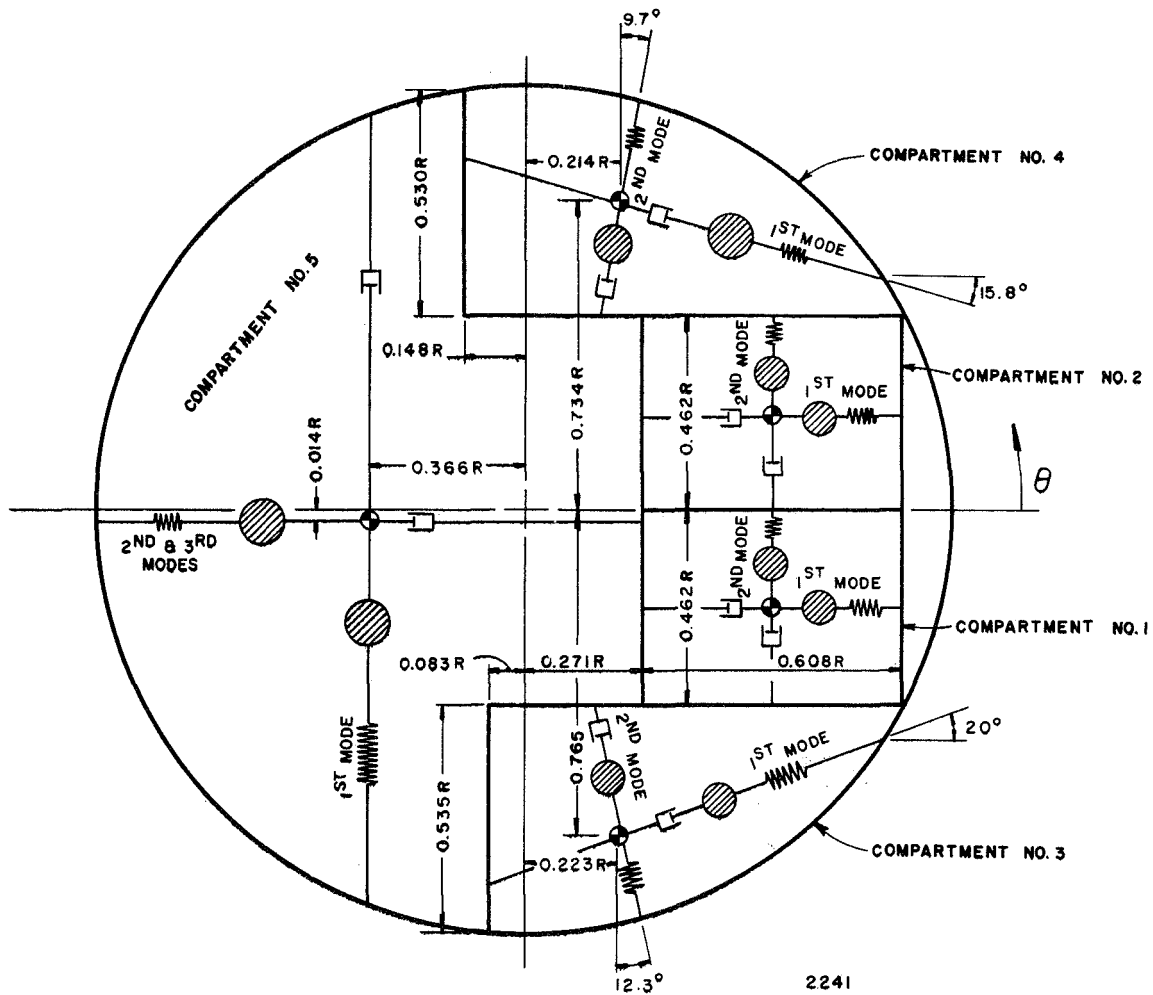


Figure 10. Orientation of Mechanical Models for Complete Tank

IV. MOMENT OF INERTIA FOR ROLL EXCITATION

The objective of this series of roll-excitation tests was the determination of the polar mass moment of inertia of the liquid for a vertical axis through the geometric center of the cylindrical tank.

Referring to the mechanical model shown in Figure 2, roll excitation will cause torques on the tank not only because the slosh masses will oscillate but also because both the rigidly attached masses and the slosh masses will participate in the rigid body motion of the tank. In general, however, the torques produced by the model's rigid body motion will not equal the rigid body torques measured in roll excitation tests. To bring the model and the tests into correspondence, an additional moment of inertia must be added to the model; this can be accomplished by locating a massless disc having a polar moment of inertia, I_o , on the tank axis. (Since the disc has no mass, it has no influence on the mechanical model for lateral excitation.) The equivalent polar moment of inertia of the liquid acting as a rigid body is, then,

$$I_{\text{equivalent}} = I_o + \sum m_n \rho_n^2 + \sum m_o \rho_o^2 \quad (6)$$

The last two terms in Equation (6) account for the transfer moment of inertia of the slosh masses and the rigidly attached masses in the various compartments. The quantity that is to be determined in this series of tests, therefore, is $I_{\text{equivalent}}$.

Test Procedures

Previous analyses of the sloshing in a cylindrical tank divided in quarters for roll excitation have shown that the rigid body part of the torque is identical to that which would occur if the free surface wave motion were suppressed [10]. Generalizing this result, it may be concluded that measuring the torque on an arbitrarily compartmented tank during a roll excitation when there is no wave motion will allow $I_{\text{equivalent}}$ to be computed.

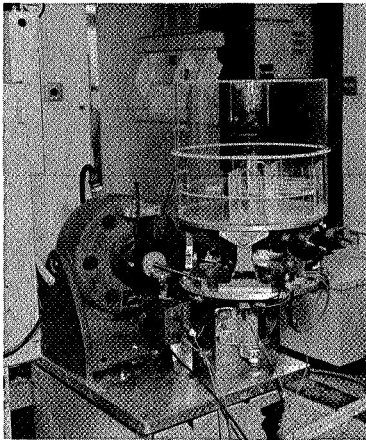


Figure 11. Test Setup for Roll Excitation Tests

The method used here to suppress the waves was to fit the tank with a rigid lid that just contacted the free surface. Since the viscosity of the water is not zero, the lid induces viscous stresses, as do also the walls, and thus influences the amount of liquid set in motion. Nonetheless, previous experimental determinations of the equivalent moment of inertia for pitching motions agreed very well with theories that assumed ideal (zero viscosity) liquids [11]; this is both because the viscosity is small and because an oscillatory excitation does not allow the viscous action to penetrate very far into the body of the liquid. As will be seen, here also the viscosity had only a negligible influence on the results.

The apparatus constructed to provide the desired simple harmonic roll excitation and to measure the resulting torques is shown in Figure 11. It consisted of an aluminum base free to rotate about an axle through its center, an electrodynamic shaker which, because of the off-center attachment to the base, gave a rotary motion to the base, a dynamometer system (connecting the tank to the base) which measured the torque, and an arrangement of balance weights used to cancel electrically the dynamometer signal of the empty tank.

Equivalent Moment of Inertia

With the compartment doors *closed* results of the roll excitation tests are shown in Figure 12. The upper part of the figure presents the equivalent rigid mass of liquid set into motion by the simple harmonic

roll excitation ($\theta_0 e^{2\pi if t}$) as a function of the excitation frequency f and roll amplitude, θ_0 . This is the mass associated with the polar moment of inertia of a rigid cylinder (having a radius equal to R_0) giving the same torque as that measured in the tests for the same roll excitation. For a given liquid level, the results depend very little on either the amplitude or the frequency of the excitation. Furthermore, since the amount of liquid motion due purely to viscous stresses is proportional to $\sqrt{f/\nu}$, changing the excitation frequency, f , is equivalent to changing the viscosity, ν [12]. Consequently, it can be deduced that viscosity does not influence $I_{\text{equivalent}}$ to any noticeable degree, most of the liquid motion being caused by the compartment walls themselves. (In an uncomparted tank, of course, the small amount of liquid set into motion by a roll excitation is due entirely to viscous stresses.)

By using the average of the equivalent rigid mass for each liquid level, the average polar moment of inertia for that level can be computed; it is $1/2 m R_0^2$ where m is the equivalent rigid mass. The results are shown in the lower part of Figure 12; the vertical axis on the graph is the ratio of $I_{\text{equivalent}} = 1/2 m R_0^2$ to the polar moment of inertia of the liquid if it were "frozen" ($1/2 M R_0^2$ where M is the actual mass of liquid in the tank). As can be seen, $I_{\text{equivalent}}$ increases almost linearly with the filling level from a value of 55% of the frozen moment of inertia at low liquid levels to about 70% for a full tank.

Figure 13 shows similar results for the tank with the compartment doors closed. As might be expected, there is very little difference between the two cases.

With these results, the equivalent mechanical model for both lateral and roll excitations can be completely formulated.

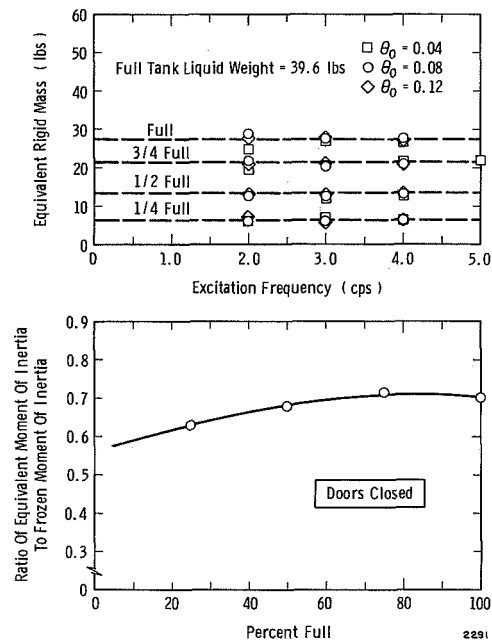


Figure 12. Polar Moment of Inertia with Doors Closed

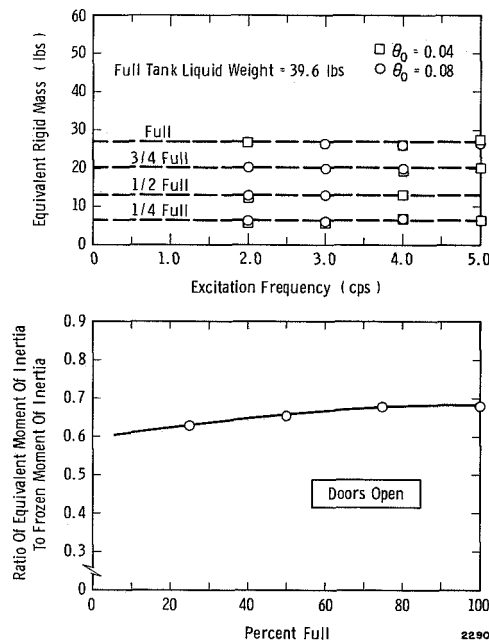


Figure 13. Polar Moment of Inertia with Doors Open

V. COMPARISON OF COMPLETE MECHANICAL MODEL WITH TESTS

Slosh forces, moments, and torques predicted by the mechanical model for the complete tank (Figure 10) are compared in this section to test results for both lateral and roll excitation. The lateral excitation tests were run using the apparatus shown in Figure 4 and the roll excitation tests with the one shown in Figure 11. Several liquid levels were employed; the results presented here for the half-full tank are representative of all the tests. The lateral and roll excitation amplitudes were, respectively, $x_o = 0.005$ in. and $\theta_o = 0.08^\circ$.

Lateral Excitation

Comparisons were made with both the doors open and the doors closed in all the compartments. For both cases, the force, F , and moment, M predicted by the mechanical model were computed from the following equations:

$$F = -(2\pi f)^2 \mathcal{M} x_o \left\{ 1 + \sum \frac{m_n}{\mathcal{M}} \cos^2(\theta_m - \theta) \left[\frac{\left(\frac{f}{f_n}\right)^2}{1 - \left(\frac{f}{f_n}\right)^2 + 2i\gamma_n \left(\frac{f}{f_n}\right)} \right] \right\} e^{2\pi i f t} \quad (7)$$

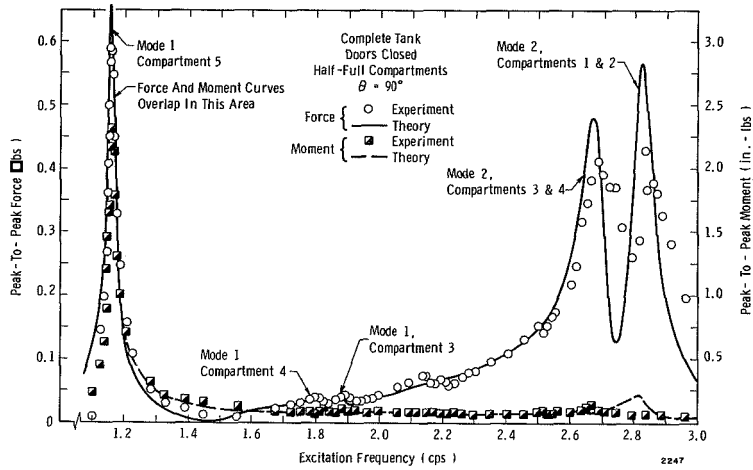
$$M = -(2\pi f)^2 \mathcal{M} x_o h \left\{ \sum \frac{m_n}{\mathcal{M}} \cos^2(\theta_m - \theta) \left[\frac{\frac{g}{(2\pi f_n)^2 h} + \frac{h_n}{h} \left(\frac{f}{f_n}\right)^2}{1 - \left(\frac{f}{f_n}\right)^2 + 2i\gamma_n \left(\frac{f}{f_n}\right)} \right] \right\} e^{2\pi i f t} \quad (8)$$

where, as before, θ is the angle specifying the direction of the excitation. The summation signs in the equation imply that all eleven modes in the model are considered. Equations (7) and (8) are quite similar to the equations for an individual compartment, the main difference being that the total mass in the tank, \mathcal{M} , is used instead of the mass in an individual compartment, m_T .

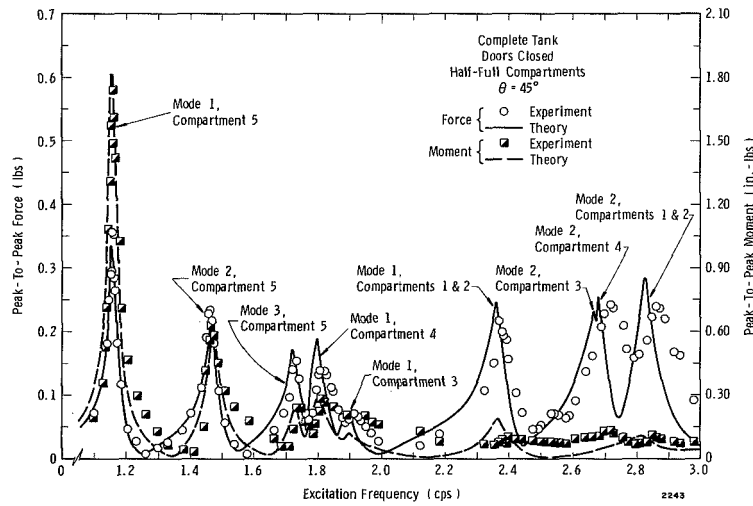
With the doors *closed*, comparisons of tests and the model are shown in Figure 14 for directions of excitation equal to 90° , 45° , and 0° . Although some minor high-order modes in Compartment 5, not accounted for in the model, show up in the frequency range of interest, the agreement is generally very close. Recall that except for Compartment 5 the mechanical model was developed from data obtained in much larger tanks than the compartments of the scale-model. Consequently, the close comparison substantiates the nondimensional scaling parameters presented in Figures 5 through 8 and thus verifies the mechanical model.

With the doors *open*, comparisons of tests and model are not quite so close, as might be expected.* Nonetheless, the agreement is still fairly good, as can be seen in Figure 15. The major discrepancies are of two kinds: shifts in the experimental natural frequencies and decreases in the experimental forces and moments. The shifts in the natural frequencies are not large, never amounting to more than about 0.05 cps for the primary modes. However, the shifts are usually to higher frequencies, which at first sight is perplexing since an open door should increase the effective size of an individual compartment and thus decrease its natural frequency. In fact, this does happen to the second mode for Compartment 5, the lowest frequency mode along the $\theta = 0^\circ$ axis; this mode, which involves a lot of wave motion to and from the two doors in Compartments 1 and 2 along the 0° axis, is shifted downward from about 1.75 to about 0.8 cps, with a large reduction in its slosh force and moment. A valid method of accounting for the natural

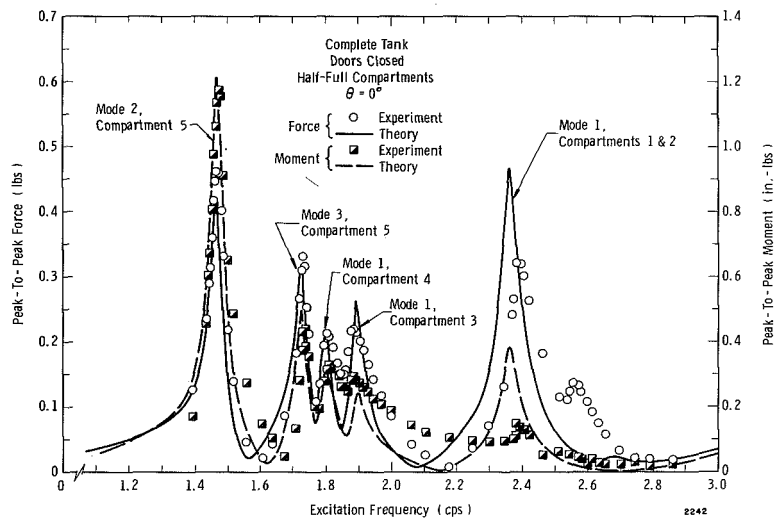
*Only the theoretical force curves are shown in these figures; the moment curves are similar. Both sets of curves, in fact, are the same as those shown in Figure 14.



a. Direction of Excitation = 90°

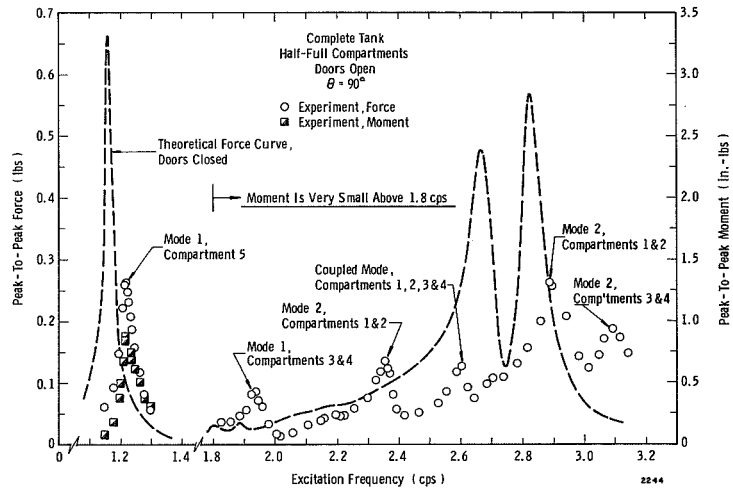


b. Direction of Excitation = 45°

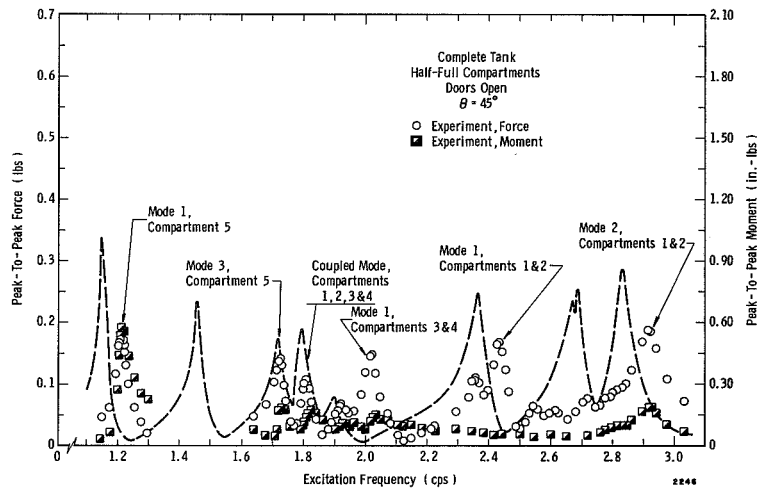


c. Direction of Excitation = 0°

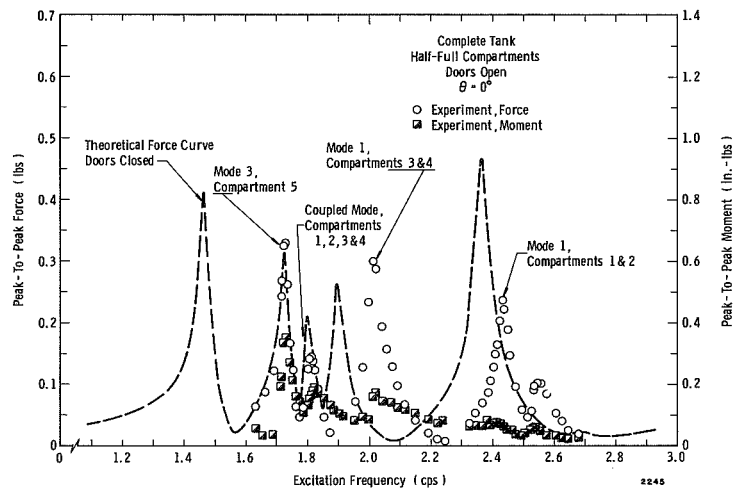
Figure 14. Comparison of Mechanical Model for Complete Tank to Test Results--Lateral Excitation $x_o = 0.005$ in., Doors Closed



a. Direction of Excitation = 90°



b. Direction of Excitation = 45°



c. Direction of Excitation = 0°

Figure 15. Comparison of Mechanical Model for Complete Tank to Test Results—Lateral Excitation $x_o = 0.005$ in., Doors Open

frequency shifts has not been determined; in most cases, however, the shifts should be negligible. On the other hand, the decreases in the forces and moments, which are primarily caused by the radiation of wave energy from an individual compartment to an adjacent one, thereby increasing the apparent damping, can be accounted for by doubling the damping coefficients, γ_n , obtained from tests with the doors closed (Figures 5 through 8). This will bring the predicted force and moment and the measured force and moment for nearly all the important modes into satisfactory agreement.

Roll Excitation

The torque exerted on the tank by the equivalent mechanical model shown in Figure 4 for a roll excitation can be computed by adding a massless disc having a polar moment of inertia I_o at the geometric axis, as mentioned earlier, and by accounting for the offset distances of the masses from the axis. Using a consistent set of positive directions for acceleration and torque, the result is

$$T = -\frac{1}{2} \mathcal{M} R_o^2 \theta_o (2\pi f)^2 \left\{ \frac{I_{\text{equivalent}}}{\frac{1}{2} \mathcal{M} R_o^2} + 2 \sum \frac{m_n}{\mathcal{M}} \left(\frac{\ell_n}{R_o} \right)^2 \left[\frac{\left(\frac{f}{f_n} \right)^2}{1 - \left(\frac{f}{f_n} \right)^2 + 2i\gamma_n \left(\frac{f}{f_n} \right)} \right] \right\} e^{2\pi i f t} \quad (9)$$

where use has been made of Equation (6):

$$I_{\text{equivalent}} = I_o + \sum m_n \ell_n^2 + \sum m_o \ell_o^2$$

From the geometry of Figure 12, the distances ℓ_n in Equation (9) are computed to be:

Compartments 1 and 2:	First Mode	$\ell_1 = 0.231 R_o$
	Second Mode	$\ell_2 = 0.575 R_o$
Compartment 3:	First Mode	$\ell_1 = 0.795 R_o$
	Second Mode	$\ell_2 = 0.051 R_o$
Compartment 4:	First Mode	$\ell_1 = 0.766 R_o$
	Second Mode	$\ell_2 = 0.088 R_o$
Compartment 5:	First Mode	$\ell_1 = 0.366 R_o$
	Second Mode	$\ell_2 = 0.014 R_o$
	Third Mode	$\ell_3 = 0.014 R_o$

(The ℓ_n are the perpendicular distances from the center of the tank to the line of action of the spring-dashpot for the m_n mass.)

Comparisons of the peak-to-peak torque from Equation (9) and the tests are shown in Figure 16, for the tank with doors *closed*. Once again, the agreement is excellent.

With the doors *open* comparisons are shown in Figure 17. Here, again, there are slight shifts in the experimental natural frequencies and decreases in the torques from the results with the doors open. But, again, the torque prediction of the model can be brought into satisfactory agreement by doubling the damping coefficients, γ_n .

Tests with the Liquid Level Above the Compartments

A few tests were conducted for both lateral and roll excitation when the liquid level was above the top of the compartments. These tests were rather cursory and designed primarily to determine if slosh resonances in individual compartments still existed for such liquid levels. The results are shown in Figure 18, for a level of liquid above the top of the compartment by a distance equal to one-fourth the compartment height; that is, $h \approx 6.35$ inches. For greater depths, the sloshing strongly resembled that occurring in a

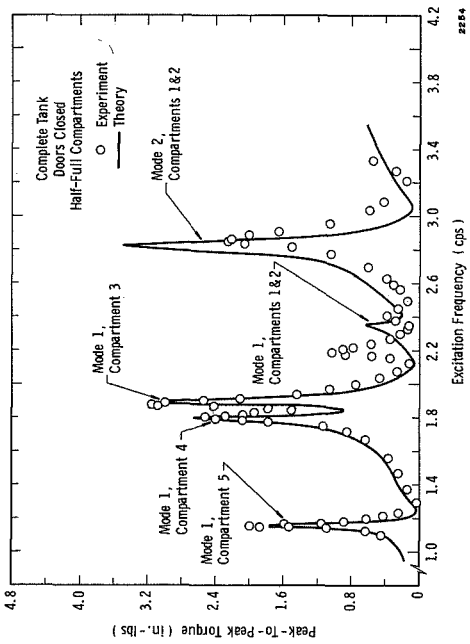


Figure 16. Comparison of Mechanical Model for Complete Tank to Test Results—Roll Excitation $\theta_0 = 0.08^\circ$, Doors Closed

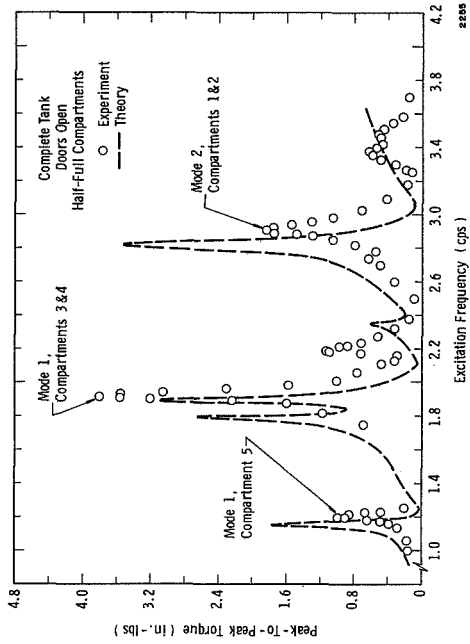
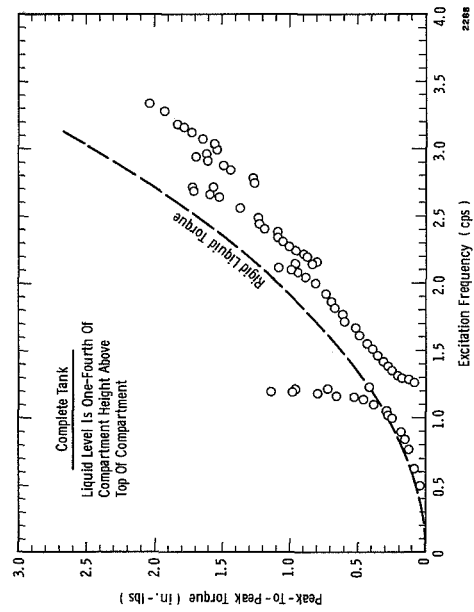
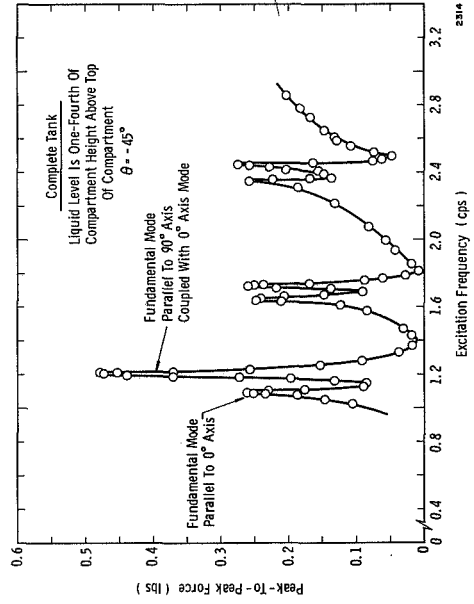


Figure 17. Comparison of Mechanical Model for Complete Tank to Test Results—Roll Excitation $\theta_0 = 0.08^\circ$, Doors Open



a. Lateral Excitation, $x_0 = 0.005$ in.



b. Roll Excitation, $\theta_0 = 0.08^\circ$

Figure 18. Liquid Level Above Top of Compartments

flat-bottom cylindrical tank with no compartments; thus, the compartmentation has no influence at these depths.

As the figures show, individual compartment resonances still occurred for $h = 6.35$ in., although with a greatly increased damping. However, the dominant resonance was similar to the fundamental mode in a cylindrical tank. It is also interesting to note that the rigid body motion of the liquid accounts for most of the roll torque shown in Figure 18b; the rigid body torque shown here was computed from Equation (9) by neglecting the resonance terms and setting $I_{\text{equivalent}}$ to seven-tenths of $0.5 \mathcal{M} R_o^2$, where \mathcal{M} in this case is the total liquid mass when the liquid level just fills the compartments; see Figures 14 or 15.

The mechanical model is not meant to apply to liquid levels above the compartments; thus, comparisons are not shown. Presumably, the sloshing at these levels can be controlled by standard baffles.

VI. CONCLUSIONS

The equivalent mechanical model for the AS-209 "workshop" mission developed during the program described herein has been shown to adequately represent the propellant sloshing for both lateral and roll excitations. By including an appropriate moment of inertia, the model can also be made valid for pitching or yawing motions; this was not felt to be worthwhile inasmuch as the contribution of this inertia to the slosh moment in most situations is small compared to the moment of the masses already included in the model.

The slosh masses and natural frequencies for all eleven distinct modes included in the model were shown to be nearly independent of the excitation amplitude; that is, they were not nonlinear parameters. However, the heights of the slosh masses above the center-of-mass of the propellant and the viscous damping for each slosh mode did exhibit some amplitude dependence. Of all the model parameters, the viscous damping coefficients are perhaps subject to the most uncertainty since no theory exists that can be used to verify the computed values for any of the compartments.

Slosh force and moment predictions of the mechanical model for lateral excitation compared very well with test results when the compartment doors were closed. When the doors were open, there was an apparent increase in the viscous damping by a factor of about two and a slight increase in the natural frequencies. Slosh torque predictions for roll excitation also agreed excellently with tests when the compartment doors were closed; similar discrepancies as arose in the lateral excitation were also exhibited during roll when the doors were open. In all cases, however, the mechanical model gave an adequate representation of the slosh dynamics.

Two of the most important results of the program are that, during roll excitation, between five-tenths and seven-tenths of the liquid propellant participates in the rigid body motion of the tank, and large, resonant slosh torques are exerted on the tank. These conclusions are in contrast to the liquid motions in a noncompartmented cylindrical tank, for which the liquid is essentially uncoupled from roll motions of the tank.

VII. LIST OF REFERENCES

1. Sumner, I. E., Stofan, A. J., and Shamro, D. J.: Experimental Sloshing Characteristics and a Mechanical Analogy of Liquid Sloshing in a Scale-Model Centaur Liquid Oxygen Tank. NASA TM X-999, August 1964.
2. Stofan, A. J.: Comparison of Propellant Sloshing Parameters Obtained from Model and Full-Size Centaur Liquid-Oxygen Tanks. NASA TM X-1286, September 1966.
3. Sumner, I. E., Lacovic, R. F., and Stofan, A. J.: Experimental Investigation of Liquid Sloshing in a Scale-Model Centaur Liquid Hydrogen Tank. NASA TM X-1313, November 1966.
4. Eggleston, D. M.: Atlas Fuel Tank Propellant Slosh Model Tests. Report GDC-DDE66-029, Contract AF 04(695)-514, General Dynamics Corporation, Convair Division, October 1966.
5. Eggleston, D. M.: Dynamic Stability of Space Vehicles. Volume XIV—Testing for Booster Propellant Sloshing Parameters. NASA CR-948, May 1968.
6. Dodge, F. T.: Analytical Representation of Lateral Sloshing by Equivalent Mechanical Models. Chapter 6 of *The Dynamic Behavior of Liquids in Moving Containers*, H. N. Abramson (Ed.), NASA SP-106, December 1966.
7. Abramson, H. N. and Ransleben, G. E., Jr.: Simulation of Fuel Sloshing Characteristics in Missile Tanks by Use of Small Models. *ARS Journal*, Vol 30, July 1960, pp 603-613.
8. Miles, J. W.: Ring Damping of Free Surface Oscillation in a Circular Tank. *Journal Applied Mech., Trans. ASME*, Vol 25, June 1958, pp 274-276.
9. Kana, D. D., Silverman, S., Garza, L. R., and Abramson, H. N.: Liquid Sloshing in Laterally and Longitudinally Excited Rigid Spheroids. *Proceedings of the 10th Midwestern Mechanics Conference (Developments in Mechanics)*, Vol 4, Johnson Pub. Co. (1967) pp 1275-1294.
10. Bauer, H. F.: Liquid Sloshing in a Cylindrical Quarter Tank. *AIAA Journal*, Vol 1, November 1963, pp 2601-1606.
11. Dodge, F. T. and Kana D. D.: Moment of Inertia and Damping of Liquids in Baffled Cylindrical Tanks. NASA CR-383, February 1966.
12. Schlichting, H.: **Boundary Layer Theory**, 4th Edition, McGraw-Hill Book Co., New York (1960).